



Optical color structuring via DALP-fabricated thin-film interference cavities in ZnO/SiO₂ on Si

GAUTHIER BRIERE, MATTHIAS CARNOY, MASOUD AKBARI,
BENJAMIN BORIE,* MIRA BARAKET, AND MAKSYM PLAKHOTNYUK

ATLANT 3D, Mårkaervej 2B, 2630 Taastrup, Denmark

*bbor@atlant3d.com

Abstract: We present a method for generating structural colors using direct atomic layer processing (DALP) to fabricate thin-film interference cavities made of ZnO and SiO₂ on silicon. By locally depositing successive layers and thus varying ZnO thickness from a few nanometers up to 150 nm, we achieve tunable reflective colors via depth modulation. The asymmetric interference cavities produce vivid hues through optical interference. Rigorous coupled-wave analysis simulations accurately predict the reflectance spectra, closely matching experimental results. Mapping the colors on the CIE 1931 diagram confirms agreement with design targets. A DALP-based, lithography-free approach enables fast prototyping of spatially controlled structural color filters.

© 2026 Optica Publishing Group under the terms of the [Optica Open Access Publishing Agreement](#)

1. Introduction

Color filters based on Fabry-Pérot (FP) optical cavities have been a deep and well-known topic of research. We can find their use in a large field of application from display to energy storage devices [1]. Structural color generation via thin film interferences presents several advantages over pigmentation-based coloration device, including higher durability, and a potential extreme miniaturization [1,2]. Many conventional approaches to structural color rely on nanostructured metasurfaces or plasmonic resonators, using principles such as guided mode resonance or Mie scattering. While those structures can produce high color saturation and resolution, they typically require complex fabrication steps such as lithography and etching [3]. In contrast, planar FP cavities composed of dielectric thin films and metals provide an attractive lithography-free and etching free way to color filtering [2,4–7].

Generally, a FP filter consists of a spacer layer sandwiched between two reflecting interfaces. Traditional designs often use metallic mirrors, for example an ultra-thin dielectric layer between two metal films can create a resonant cavity with a tunable color response. Fan et al. demonstrated a transmissive FP color filter using a semiconductor (IGZO) spacer between Ag mirrors, achieving a full spectrum of colors by varying the spacer thickness from ~80 nm to 180 nm.

In the present work, we explore a lithography-free thin-film interference color filter structure consisting of ZnO and SiO₂ thin films on a silicon substrate. ZnO is a wide-bandgap semiconductor (e.g. ≈ 3.3 eV) that is transparent in the visible and has a relatively high refractive index (~ 2.0), making it an effective optical spacer material. SiO₂ has a lower refractive index (~ 1.45) and serves as a stable dielectric layer and part of the cavity structure. The silicon substrate ($n \sim 3.7$ with some absorption in visible) acts as a semi-reflective, absorbing backing, analogous to the broadband absorber design. By combining these materials in a simple stack (ZnO/SiO₂ on Si), we create a thin-film interference cavity that produces reflective structural color without the need for any metallic mirror. The bilayer stack was chosen as a proof-of-concept interference cavity for DALP in this application that can be easily realized by one deposition pass on a standard silicon substrate. The color tuning mechanism in our design is the variation of the ZnO layer thickness d_{ZnO} , as the ZnO spacer thickness increases, the interference condition shifts the dominant reflected wavelength in a controlled manner. A key novelty of this work is the

fabrication method. We employ Direct Atomic Layer Processing (DALP), a recently developed additive microfabrication technique, to deposit the ZnO in a spatially selective manner. DALP is essentially a form of micro-localized Atomic Layer Deposition (ALD) that enables on-demand patterning of materials with atomic layer precision.

Unlike conventional ALD which uniformly coats entire substrates, DALP uses a microreactor nozzle to deliver precursor gases to specific regions of the substrate. This allows us to “print” different thicknesses of ZnO in designated pixel areas across the sample, thereby directly writing a multicolored pattern without any lithographic masking. The technique offers extremely fine control over film thickness with a vertical resolution on the order of a single ALD cycle, i.e. ~ 0.2 nm and can accommodate multiple materials by switching precursors.

The micronozzle used in that work is on the order of a few hundred μm s (approximately $350 \mu\text{m}$ feature size), which is sufficient for creating individual color test patches and was already demonstrated to be improved to tens of μm s or smaller in recent iterations. By leveraging DALP, we drastically simplify the fabrication workflow for structural color filters which traditionally might require deposition of films followed by photolithography to define different thickness regions. This is replaced by a single-step printing of the desired thickness pattern. For comparison, the 3×3 mm ZnO squares of 10 different thicknesses on sample 1 only took 11 uninterrupted machine hours to deposit using DALP, whereas doing the same number of samples using thermal ALD + lithography would have taken 10 complete lithography-deposition-liftoff or deposition-lithography-etch cycles. It is also possible to do it in 4 cycles by using combinatorial deposition and combining several depositions on each square at the expense of compromising thin film quality.

In the following, we present the development and characterization of these DALP-fabricated optical color structures. We first describe the DALP fabrication process and the specific sample structures produced. We then detail the optical modeling approach using Rigorous Coupled-Wave Analysis (RCWA) to predict the reflectance spectra for various ZnO thicknesses. Next, we provide experimental validation through reflectance spectroscopy measurements of the fabricated samples, comparing the results to simulations. We also convert the spectral data to CIE 1931 chromaticity coordinates to objectively quantify the perceived colors and demonstrate concordance between simulation and experiment. Finally, we discuss the implications of this technology for photonic device fabrication, including the advantages and current limitations of DALP for optical applications, and we conclude with a summary of key findings and outlook.

2. Fabrication method

The thin-film interference cavity structures were fabricated using ATLANT 3D’s Direct Atomic Layer Processing system. The system employs a microfluidic ALD print-head that can deposit thin films in user-defined patterns by moving the substrate under the print-head in a programmable fashion.

The process sequentially delivers precursor and reactant gases through the miniaturized reactor onto the substrate only at the intended locations (Fig. 1), achieving a selective area deposition with the typical self-limiting surface reactions of ALD. The result is a layer-by-layer additive deposition.

The SiO_2 layer thickness was kept constant, with $d = [200, 500] \text{nm}$ acting as a fixed spacer and insulating layer between ZnO and Si), corresponding to 2 fabricated samples. The variation in SiO_2 thickness allows us to investigate its influence on the optical response. The ZnO layer was printed on top in a patterned manner. We defined square patches of ZnO with lateral dimensions of a few millimeters. Each square patch was assigned a specific target thickness for the ZnO layer. Across the sample, we printed an array of such squares, with ZnO thickness ranging from few nanometers and up to 150 nm, in increments of ~ 10 – 20 nm. This range of thickness was chosen based on initial simulations to cover a wide gamut of colors across the visible spectrum.

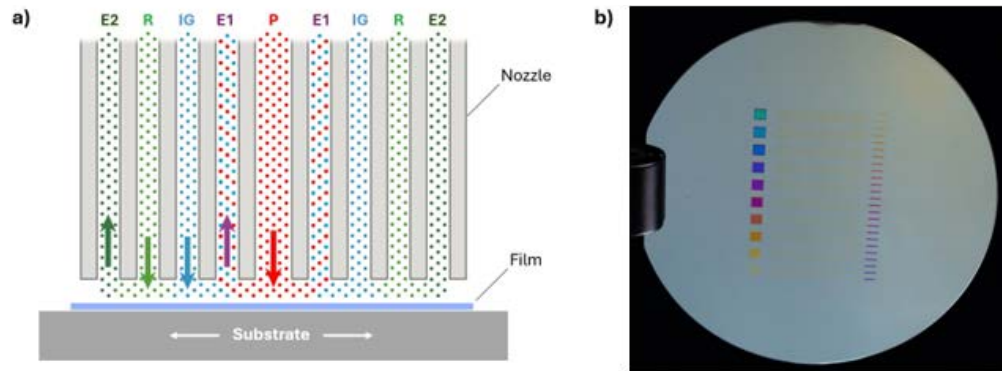


Fig. 1. (a) Schematic of the DALP micronozzle. (b) Sample 1 with ZnO deposited using DALP on a 4-inch 200 nm SiO₂ on Si wafer.

The deposition of ZnO was accomplished using a two-precursor ALD cycle repeated until the desired thickness was reached. We utilized a zinc precursor delivered in the DALP tool and an oxidizing co-reactant to produce ZnO. Each ALD cycle deposits roughly one monolayer of ZnO (approximately 0.35 Å per cycle at 150 degrees Celsius), so in the order of 500–700 cycles were required for the thickest (~150 nm) regions. The DALP system's computerized control ensures that each square region receives the correct number of ALD cycles to attain the target thickness. This is achieved by rastering the substrate when the print-head is over the designated area for a given number of passes. Because ALD is highly conformal and self-limited, the thickness uniformity within each printed patch is excellent. After deposition, the samples were handled under ambient conditions. No additional annealing was necessary, as the ZnO films were found to be adherent and of sufficient quality for optical testing, thanks to the DALP process ensuring good film continuity and density even at low deposition temperature. In summary, the fabrication yielded sample surfaces patterned with multiple thin-film interference cavity regions. Each region consists of a Si (substrate) – SiO₂ (fixed thickness) – ZnO (variable thickness) – air (top interface). Figure 2 illustrates the cross-sectional schematic of this structure.

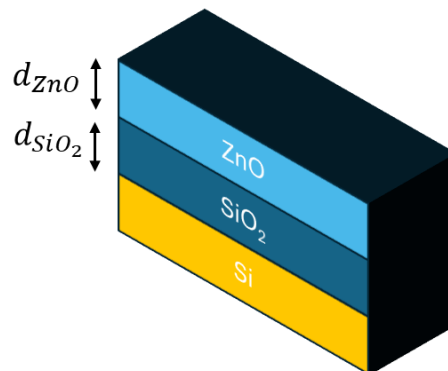


Fig. 2. Schematic of the optical cavity made of ZnO and SiO₂. The thickness of ZnO, d_{ZnO} , ranged from 0 to 150 nm. The thickness of SiO₂ is constant and two samples were prepared with $d_{SiO_2} = [200, 500]$.

3. Optical modeling and simulation

To design and understand the optical behavior of the DALP-fabricated structures, we performed optical simulations using a Rigorous Coupled-Wave Analysis (RCWA) method. RCWA is a frequency-domain electromagnetic solver well-suited for stratified media and periodic structures; in the case of a planar multilayer, RCWA effectively reduces to a thin-film interference calculation that rigorously accounts for multiple reflections and interference between all interfaces. We treated each square color patch as an infinite, laterally uniform multilayer stack (neglecting edge effects, which is reasonable since the measurement spot was focused at the center of each patch). The layer sequence in the model was air ($n = 1$) / ZnO ($d_{\text{ZnO}} = [1 - 150] \text{ nm}$, $n_{\text{ZnO}} = 1.72$) / SiO₂ ($d_{\text{SiO}_2} = [200, 500] \text{ nm}$, $n_{\text{SiO}_2} = 1.45$) / Si substrate (semi-infinite, the refractive index was taken from ANSYS library). Refractive indices for ZnO, SiO₂, were assumed constant over the visible range, confirmed by our ellipsometry data provided in the [Supplement 1](#). Using these parameters, we computed the reflectance spectra at normal incidence for each ZnO thickness of interest. The RCWA simulation effectively calculates the fraction of incident light (assumed unpolarized and at normal incidence) that is reflected by the multilayer, as a function of wavelength. We note that because the Si substrate is absorbing, the thin-film interference resonance is damped, i.e. the reflectance spectra do not reach 100% or 0% reflectance extremes, but rather moderate contrast interference. This damping, however, is beneficial for producing more angle-insensitive color, as it broadens the spectral features. From the RCWA results, we predicted that by varying ZnO thickness from 0 to 150 nm, one could achieve reflectance peaks that span the entire visible range. The precise spectral behavior also depends on the SiO₂ thickness, the two different sample designed with different SiO₂ thickness, show slightly different baseline reflectance and resonance positions (Fig. 4(a)(c)). However, in both cases, the trend of red shifting with increasing ZnO thickness holds. We also simulated the color appearance of the reflected spectra, as function of the incident angle of the source, by converting each spectrum to an RGB color under standard illumination, using a built-in function in the ANSYS optics suite, as referenced in Fig. 3. These simulations indicated a gradual change in perceived color from cyan/blue at small ZnO thickness to green, yellow, and red at the largest thickness, confirming the viability of thickness-tuned structural coloration.

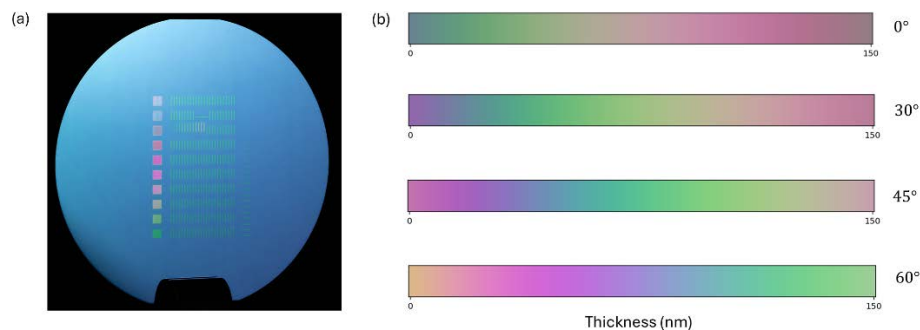


Fig. 3. (a) A near-normal incidence angle photograph of ZnO structures on Sample 2 (4-inch 500 nm SiO₂ on Si wafer). (b) The reflected color from the ZnO on Sample 2 with $d_{\text{SiO}_2} = 500 \text{ nm}$ was numerically calculated using STACK Solver from ANSYS Optics Suite.

4. Experimental validation

After fabrication, the samples were characterized to verify their optical performance. We measured the reflectance of each ZnO patch using a fiber-coupled spectrometer system from Thorlabs. A broadband white LED light source provided illumination in the 400–700 nm range.

The light was directed onto the sample at near-normal incidence. The reflected light from the sample was collected with a lens and delivered via optical fiber to the calibrated spectrometer. The spot size of the measurement beam was about 1 mm, comfortably within the area of each ZnO patch, ensuring that only one thickness region was measured at a time. A reference measurement on a broadband mirror was used to normalize the reflectance. The measured reflectance spectra for several representative ZnO thicknesses at normal incidence are shown in Fig. 4. Each spectrum exhibits distinct features that shift with the ZnO layer thickness. As the ZnO thickness increases to tens of nanometers, a pronounced dip in reflectance emerges in the shorter wavelengths (blue), causing the reflected color to shift towards the longer wavelengths. For instance, the measured patch (Fig. 4(c)) with ~50 nm ZnO showed a minimum reflectance around ~480 nm and higher reflectance in the red, yielding a yellowish reflected color. Further increasing ZnO thickness to ~100 nm moved the interference dip into the green part of the spectrum, so that the reflectance was higher at both blue and red ends, resulting in a magenta hue. At the maximum ZnO thickness around 150 nm, the main reflectance dip shifted to ~620–650 nm (the red region), meaning red light was not reflected, while shorter wavelengths (blue green) were relatively more reflected – this gave the patch a blue-green (turquoise) appearance.

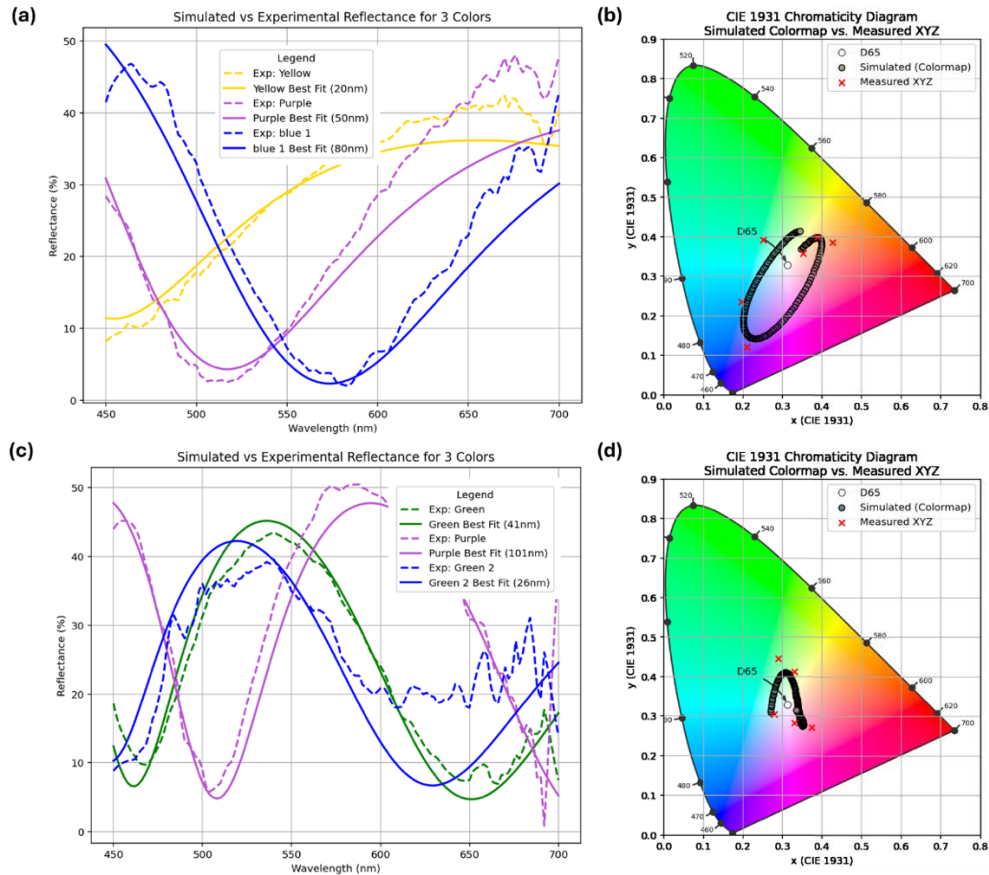


Fig. 4. The experimental Reflectance curves and the color point located on the color map were measured for different sets of squares. The reflectance curves were fitted with a RCWA model of a cavity with different SiO_2 thickness, respectively, (a)(b) $d_{SiO_2} = 200\text{ nm}$ and (b)(c) $d_{SiO_2} = 500\text{ nm}$.

Interestingly, as the ZnO thickness increased beyond a certain point, the sequence of colors did not simply follow a linear rainbow; instead, because of the multiple-beam interference in a two-layer system, there were alternating zones where one part of the spectrum or another was suppressed. Nonetheless, all colors produced were vivid and easily distinguishable, confirming that the thin-film interference cavity approach functions as intended. To quantitatively compare with the design, we fitted the measured reflectance curves using the RCWA model. For each measured spectrum, we adjusted the ZnO layer thickness in the simulation to best match the spectral positions of the reflectance minima and maxima. Figure 4 shows a representative comparison between measured and simulated reflectance for two extreme cases. The RCWA-generated spectra (dashed lines) align very well with the experimental data (solid lines). The slight discrepancies can be attributed to factors such as surface roughness (which can cause a minor diffuse scattering loss not accounted in the ideal model) and minor non-uniformity in the film thickness. This level of agreement between measurement and simulation validates both the optical model and the precision of the fabrication method. Each square exhibited a uniform color to the naked eye, with sharp boundaries between different colored squares. The ability to directly see the color difference is an important confirmation that the structural color effect is strong enough for practical visibility under ambient light.

While spectral reflectance plots provide detailed information about optical performance, it is often useful to distill the result into a single perceived color point. We therefore converted the reflectance spectra of each ZnO thickness into CIE 1931 chromaticity coordinates (x , y). This conversion was done by measuring the reflectance spectrum automatically converting it to XYZ coordinates in the color space, through the Thorlabs Software ThorSpectra, using the Color analysis tool. The resulting chromaticity points for representative samples are plotted on the CIE 1931 diagram in Fig. 4. We observed a continuous trajectory of color points as the ZnO thickness was varied. Starting from the thinnest ZnO (essentially the point for the SiO₂/Si baseline), the chromaticity was in the cyan-blue region of the diagram (with coordinates roughly around $x \sim 0.25$, $y \sim 0.30$). As the thickness increased to around 50–60 nm, the point moved towards the green-yellow region ($x \sim 0.38$, $y \sim 0.50$ for a yellowish appearance). With further increases in ZnO, the chromaticity looped towards magenta (for intermediate thickness ~ 100 nm, we got $x \sim 0.32$, $y \sim 0.22$ indicating a purple-pink tint). Finally, at the largest thickness ~ 150 nm, the point went back toward blue green ($x \sim 0.20$, $y \sim 0.35$). This non-linear path in the CIE diagram reflects the multi-peaked nature of the reflectance spectrum and the fact that the perceived color is a combination of all wavelengths. Notably, the colors achieved are reasonably saturated but not at the extreme perimeter of the CIE horseshoe; this is expected because the reflectance is not monochromatic but rather has a band-pass/band-stop shape of finite width. Nevertheless, the covered range of chromaticity is quite broad – it spans from cyan to yellow to magenta, covering a significant portion of the standard sRGB color triangle. This indicates that our structural color patches can reproduce a wide variety of hues. We also computed the chromaticity for the simulated spectra (RCWA-predicted reflectance for each thickness). The simulated color closely overlapped the experimentally measured points on the CIE diagram. The maximum difference in (x , y) between simulation and experiment for any given thickness was on the order of Δx , $\Delta y \sim 0.02$ or less, which is a small color difference barely perceptible to the eye. This further confirms that our optical model is accurately capturing the color performance. The slight differences can arise from the same factors mentioned earlier (small errors in the shape of the spectrum). Importantly, the direction of hue shift with thickness is the same in both simulation and experiment, and a designer could reliably use the simulation to predict what thickness yields a desired target color in CIE space. The CIE mapping exercise thus provides a good summary and verifies that the DALP-fabricated structures produce intended colors, and it allows one to communicate the results in standard colorimetric terms.

In a practical scenario, one could pick a target chromaticity (for example, a company logo color) and use the established thickness-to-color mapping to directly print that color using the DALP process on a substrate.

5. Discussion

The successful fabrication and validation of these structural color filters highlight several notable points regarding both the manufacturing technique and the optical design.

First the manufacturing advantages, DALP-based fabrication proved to be a robust method for creating multilayer thin-film optical devices. By eliminating photolithography and etching steps, we dramatically simplified the process flow for producing patterned optical coatings. All that is required is a suitable substrate and precursor chemicals; the pattern is defined purely in software and executed by the DALP printer. This digital approach means that producing a different color pattern (or even a full-color image comprised of many different thickness regions) is as straightforward as modifying the print file – no masks or new tooling needed. The turnaround time for iterating a design is therefore shortened, which is highly advantageous in research and prototyping of optical components. This opens the door to fabricating more complex optical structures, such as multi-layer dielectric mirrors or hybrid metal-dielectric devices, in a single continuous process. The vertical precision of atomic layer deposition also means we can finely tune resonance conditions with sub-nanometer accuracy, far better control than most other thin-film deposition techniques. The primary limitation of the current DALP technology is the lateral resolution ($\sim 100\text{--}400\ \mu\text{m}$ feature size), which is governed by the size of the microreactor nozzle and the diffusion of precursors. However, ongoing developments are aiming to reduce the feature size to tens of μm s and eventually to the micron scale. As the resolution improves, one could envision DALP producing pixelated color filter arrays for imaging sensors or even direct-write color holograms.

Second, the optical results show that our $\text{ZnO}/\text{SiO}_2/\text{Si}$ cavity design can achieve a wide range of colors, but how do they compare to alternative structural color technologies? Traditional pigment color filters typically provide very high saturation (narrowband spectral responses) but are not dynamically tunable. Nanostructured plasmonic filters can produce extremely saturated colors with sub-micron pixel sizes, however, they still require high-resolution nanolithography of metallic patterns, which makes large-area, low-cost manufacturing challenging. Dielectric metasurface filters (e.g., using high-index resonators) can mitigate loss and reach high efficiency, yet fabricating them requires e-beam lithography or advanced etching. Our approach, using a planar thin-film interference cavity on an absorbing substrate, yields colors of moderate saturation and reflectance (peak reflectance on the order of 20–40% in our case, limited by the one-sided mirror design). The advantage is that the colors are quite independent of viewing angle: since the cavity Q-factor is low (due to absorption in Si and the low reflectivity of interfaces), the reflected hue does not shift dramatically with angle – a viewer can move over a wide range ($\sim \pm 40^\circ$ or more) and still perceive a similar color, which is a desirable property for displays or decorative coatings, such as ALD coating in the watch industry [8,9]. This angle robustness is a known benefit of lossy-cavity designs [1], and we effectively leverage it with the Si substrate acting as the absorber. If higher reflectance or more vivid colors are required, one could integrate a back reflector (for instance, add a metal layer beneath the SiO_2).

Finally, the use of RCWA simulation to guide and confirm the experiments underscores the importance of accurate optical modeling. Because DALP allows precise control over geometry, it is feasible to reliably design optical responses beforehand. The small discrepancies observed (few nanometers in wavelength or a few in % reflectance) could be further minimized by incorporating more detailed models of, e.g., surface roughness or slight grading of material at the interfaces. In practice, we see that a simple planar model sufficed, which is helpful for rapid design. We also found that the presence of the fixed SiO_2 layer adds an additional tuning parameter: for instance,

by adjusting the SiO₂ thickness, one could shift the entire color palette or achieve certain baseline color (with no ZnO) as desired. In our two sample sets, the thicker SiO₂ substrate produced slightly different hues than the thinner one for the same ZnO thickness – this could be used as a design feature.

6. Conclusion

We have presented a comprehensive study on optical color structuring using a DALP-based fabrication process, successfully demonstrating Fabry–Pérot type structural color filters made of ZnO and SiO₂ on silicon. The work balanced the development of an advanced manufacturing technique with rigorous optical analysis and validation. Through the DALP approach, we directly printed thin-film interference cavities of varying ZnO thickness, achieving a palette of reflective colors without any lithography or masking steps. The experimental measurements of reflectance spectra for these structures showed clear thickness-dependent color tuning, in line with the principles of thin-film interference. By employing RCWA simulations, we were able to accurately predict optical behavior and match it to the observed results, lending confidence to both the fabrication precision and the optical model. Furthermore, by mapping the colors onto the CIE 1931 chromaticity diagram, we quantitatively confirmed that the DALP-fabricated devices produce well-defined colors that correspond closely to design expectations. In conclusion, the combination of DALP fabrication and thin-film interference cavity design constitutes a powerful methodology for creating custom optical filters and color devices. This study serves as a proof-of-concept that DALP can be used not only for electronic materials and prototyping but also for photonic structures requiring nanoscale control. The ability to arbitrarily pattern material thickness at the atomic level together with inherent lateral 2D patterning unlocks new possibilities in device miniaturization and rapid prototyping. We believe this approach could be extended to a variety of applications, including on-chip optical components, reflective displays, and smart decorative surfaces. Future work will explore expanding the color gamut and efficiency of these devices, integrating additional materials (such as metallic reflectors or active layers). These outcomes may inspire further research at the intersection of advanced manufacturing and nanophotonics, driving innovation in structural coloration.

Disclosures. All authors are employees of ATLANT 3D. The authors declare no other conflicts of interest.

Data availability. Data underlying the results presented in this paper are not publicly available at this time but may be obtained from the authors upon reasonable request.

Supplemental document. See [Supplement 1](#) for supporting content.

References

1. X. Fan, S. Wang, D. Xu, *et al.*, “Ultra-Thin and Lithography-Free Transmissive Color Filter Based on Doped Indium Gallium Zinc Oxide with High Performance,” *Micromachines* **13**(8), 1228 (2022).
2. A. Shaukat, F. Noble, and K. M. Arif, “Nanostructured color filters: a review of recent developments,” *Nanomaterials* **10**(8), 1554 (2020).
3. M. A. Rahman, S. D. Rezaei, D. Arora, *et al.*, “Scaling up multispectral color filters with binary lithography and reflow (BLR),” *Nanophotonics* **13**(19), 3671–3677 (2024).
4. M. J. Uddin, T. Khaleque, and R. Magnusson, “Guided-mode resonant polarization-controlled tunable color filters,” *Opt. Express* **22**(10), 12307–12315 (2014).
5. P. Dai, Y. Wang, Y. Hu, *et al.*, “Accurate inverse design of Fabry–Pérot-cavity-based color filters far beyond sRGB via a bidirectional artificial neural network,” *Photonics Res.* **9**(5), B236–B246 (2021).
6. Z. Yang, Y. Zhou, Y. Chen, *et al.*, “Reflective color filters and monolithic color printing based on asymmetric Fabry–Pérot cavities using nickel as a broadband absorber,” *Adv. Opt. Mater.* **4**(8), 1196–1202 (2016).
7. C.-S. Park, V. R. Shrestha, S.-S. Lee, *et al.*, “Omnidirectional color filters capitalizing on a nano-resonator of Ag-TiO₂-Ag integrated with a phase compensating dielectric overlay,” *Sci. Rep.* **5**(1), 8467 (2015).
8. <https://mb.cision.com/Main/16058/2581434/883197.pdf>
9. <https://quillandpad.com/2024/04/14/coloring-watches-pvd-physical-vapour-deposition-and-ald-atomic-layer-deposition/>